Multi-photon lithography of 3D micro-structures in As_2S_3 and $Ge_5(As_2Se_3)_{95}$ chalcogenide glasses

Casey M. Schwarz[a], Shreya Labh[a], Jayk E. Barker[a], Ryan J. Sapia[a],
Gerald D. Richardson[a], Clara Rivero-Baleine[c], Benn Gleason[b],
Kathleen A. Richardson[b], Alexej Pogrebnyakov[d], Theresa S. Mayer[d],
Stephen M. Kuebler[a,b,e*]

[a]Chemistry Department, University of Central Florida, Orlando, FL 32816, USA
[b]CREOL, The College of Optics & Photonics, University of Central Florida, Orlando, FL 32816, USA
[c]Lockheed Martin, Orlando, FL 32819, USA
[d]Department of Electrical Engineering, Pennsylvania State University, University Park, PA 16802, USA
[e]Physics Department, University of Central Florida, Orlando, FL 32816, USA

*kuebler@ucf.edu; Tele: +1 407-823-3720; Fax: +1 407-823-2252; http://npm.creol.ucf.edu

ABSTRACT

This work reports a detailed study of the processing and photo-patterning of two chalcogenide glasses (ChGs) − arsenic trisulfide (As_2S_3) and a new composition of germanium-doped arsenic triselenide $Ge_5(As_2Se_3)_{95}$ − as well as their use for creating functional optical structures. ChGs are materials with excellent infrared (IR) transparency, large index of refraction, low coefficient of thermal expansion, and low change in refractive index with temperature. These features make them well suited for a wide range of commercial and industrial applications including detectors, sensors, photonics, and acousto-optics. Photo-patternable films of As_2S_3 and $Ge_5(As_2Se_3)_{95}$ were prepared by thermally depositing the ChGs onto silicon substrates. For some As_2S_3 samples, an anti-reflection layer of arsenic triselenide (As_2Se_3) was first added to mitigate the effects of standing-wave interference during laser patterning. The ChG films were photo-patterned by multi-photon lithography (MPL) and then chemically etched to remove the unexposed material, leaving free-standing structures that were negative-tone replicas of the photo-pattern in networked-solid ChG. The chemical composition and refractive index of the unexposed and photo-exposed materials were examined using Raman spectroscopy and near-IR ellipsometry. Nano-structured arrays were photo-patterned and the resulting nano-structure morphology and chemical composition were characterized and correlated with the film compositions, conditions of thermal deposition, patterned irradiation, and etch processing. Photo-patterned $Ge_5(As_2Se_3)_{95}$ was found to be more resistant than As_2S_3 toward degradation by formation of surface oxides.

Keywords: Chalcogenide glass, photonics, multi-photon lithography, microfabrication.

1. INTRODUCTION

Multiphoton lithography (MPL) is a powerful photo-patterning technique that has been used to create three-dimensional (3D) structures and functional devices in materials such as glass, polymerizable resin, or heterogeneous composites [1]. These devices have applications in optics, sensing, imaging, consumer electronics, micro-electromechanical systems, and medicine [2-4]. However, there are only a few semiconductor systems that can be directly

Advanced Fabrication Technologies for Micro/Nano Optics and Photonics IX, edited by Georg von Freymann, Winston V. Schoenfeld, Raymond C. Rumpf, Proc. of SPIE Vol. 9759, 975916
 · doi: 10.1117/12.2213030

photo-patterned. New semiconductor materials systems are needed to create structures with electronic, magnetic, thermal, optical, or mechanical function, or the ability to respond to a chemically active environment, as needed for sensing.

Chalcogenide glasses (ChGs) are semiconducting photo-patternable multi-component glasses with tunable properties such as photosensitivity, index of refraction (n), dn/dT, glass transition temperature (T_g), and coefficient of thermal expansion (CTE) [2-5]. ChGs have high optical nonlinearity, a wide infrared transmission window, and a large index of refraction, and find applications in bulk optics, photonic waveguides, sensors, and acousto-optics [2-4]. To date, the most common ChG for MPL is arsenic trisulfide (As_2S_3). MPL has been used in As_2S_3 to create 3D structures such as waveguides, photonic crystals, and nanowires [2-4, 6, 7]. However, As_2S_3 is known to degrade upon exposure to ambient air and humidity making it unsuitable for use in functional devices without coating [8].

ChG glasses containing Se and Ge offer advantages over As_2S_3 glasses. Increasing the Ge content should increase the polarizability and therefore the index of refraction of the thermally deposited films and the laser patterned structures. This is useful for creating meta-optics. The addition of Ge should also increase the mechanical toughness of the thermally deposited films and the laser patterned structures [9]. There are only a limited number of studies regarding photo-exposure and etch processing of Ge/Se-based ChGs.

This work reports a detailed study of MPL in As_2S_3 and $Ge_5(As_2Se_3)_{95}$ films and how the micro-structure, morphology, chemical networking, and appearance of the resulting features are affected by the chemical composition, deposition rate, etch processing, and the inclusion of an anti-reflective (AR) layer of As_2Se_3 between the substrate and the photo-patternable As_2S_3. MPL of micro-structures in thermally deposited $Ge_5(As_2Se_3)_{95}$ films is reported for the first time and compared to micro-structures patterned by MPL in As_2S_3 films with an AR coating. Photo-patterned $Ge_5(As_2Se_3)_{95}$ micro-structures were found to be more resistant to than As_2S_3 toward degradation by formation of surface oxides.

2. METHODOLOGY

2.1. Thermal deposition of thin films

Two types of photo-sensitive films were studied in this work: a multi-layered film consisting of As_2S_3 on an AR-layer of As_2Se_3 and a single-layered film consisting of $Ge_5(As_2Se_3)_{95}$. For the multi-layered film, a layer of As_2Se_3 was deposited first on polished silicon wafers followed by thermal evaporation of a layer of As_2S_3. The As_2Se_3 layer was deposited at a rate of 4 Å s^{-1} and had a thickness of 208 nm ± 15 nm. The As_2S_3 layer was deposited at a rate of 30 Å s^{-1} and had a thickness of 2276 nm ± 141 nm. The multi-layer film appeared silver in color. For the $Ge_5(As_2Se_3)_{95}$ film, a layer of $Ge_5(As_2Se_3)_{95}$ was deposited on polished silicon wafers. The $Ge_5(As_2Se_3)_{95}$ film was deposited at a rate of 55 Å s^{-1} - 75 Å s^{-1}, had a thickness of 511 nm ± 6.8 nm, and appeared silver in color. For the deposition of As_2S_3-on-As_2Se_3 film the substrate temperature was controlled through a water cooled stage. All films were transported in petri dishes wrapped with aluminum foil and stored in an amber desiccator to prevent unintended exposure to ambient light.

2.2. Direct laser writing and UV exposure

MPL of the film samples was conducted using a continuous-wave mode-locked femtosecond laser (Coherent-Mira, 800-nm center wavelength, 120-fs pulse duration, 76 MHz repetition rate). An acousto-optic modulator (AOM) was used for the electronic control of the intensity of the laser beam. The laser beam was directed through a beam expander to a 100×/1.4 *NA* oil-immersion objective (Nikon), which focused the beam into the film/substrate interface. A coordinate system is defined such that the substrate lies in the *xy*-plane and the beam is focused along the *z*-axis. The average power used to cross-link the films was measured at the exit aperture of the objective lens using an integrating sphere. To define the pattern, the sample was translated at a speed of 50 μm s^{-1} in the *x*-, *y*-, and *z*-axes relative to the laser beam. Single-point, nano-scale feature arrays were photo-patterned by locating the beam to a targeted (*x*,*y*)-position, exposing the region at a certain power controlled by the AOM, then translating the sample in the *z*-direction over a distance of 2 μm - 4 μm. This ensured that features were exposed throughout the entire thickness of the film. Dose arrays were used to study the exposure conditions needed to photo-pattern the films. The dose arrays consisted of

sets of sixteen arrays, each with a 9 × 9 grid of single-point exposures with a 500 nm pitch. The dose arrays were patterned over a range of average (avg) focused laser powers (0.02 mW to 1.00 mW).

2.3. Etch development

The etch durations of the As_2S_3-on-As_2Se_3 and $Ge_5(As_2Se_3)_{95}$ films were measured by immersing the films in solutions of 0.5 mol-% diisopentylamine (DIPA) dissolved in dimethylsulfoxide (DMSO) and ethanolamine, respectively, and monitored visually with a camera to identify the time required to remove the unexposed material. The same etching method and solution was used for the development of photo-patterned micro-structures. The developed micro-structures also underwent additional rinsing steps following chemical etching. For the As_2S_3-on-As_2Se_3 films the micro-structures were rinsed for 15 seconds in a fresh solution of DIPA in DMSO then immersed in IPA for 2 minutes. For the $Ge_5(As_2Se_3)_{95}$ films the micro-structures were rinsed for 15 seconds in a fresh solution of ethanolamine then immersed in IPA for 2 minutes. A scanning electron microscope (SEM, Zeiss ULTRA-55 FEG) was used to record top-down and profile images of the micro-structures. These images were used to determine the dimensions and shapes of the features so they could be correlated with film composition, processing conditions, and fabrication laser power.

2.4. Spectroscopic and optical characterization

The chemical composition of the pristine films was explored using micro-Raman spectroscopy. A Bruker Senterra micro Raman system with an average power of 10 mW and an excitation wavelength of 785 nm was also used. The incoming laser beam was focused onto the front polished surface of the sample using a 10× microscope objective (*NA* = 0.30, *WD* = 15 mm) without attenuation. The resulting focused beam diameter was 50 μm – 200 μm. The Zeiss ULTRA-55 FEG SEM was equipped for energy-dispersive X-ray spectroscopy (EDX) for elemental analysis. The index of refraction of pristine films was determined using a variable-angle ellipsometer (Woollam M2000, 0.24 μm - 1.7 μm). Focusing optics were used to characterize sample areas as small as 100 μm × 100 μm with a spectral resolution of 3 nm at visible wavelengths and 6 nm in the near infrared.

3. RESULTS AND ANALYSIS

3.1. Etch processing of films

A solution of 0.5 mol-% DIPA in DMSO was found to dissolve the as-deposited As_2S_3 material leaving behind only the As_2Se_3 layer. Visual observations revealed that a 5 minute etch time was required to completely remove the As_2S_3 layer from the multi-layered films. Additionally, the As_2Se_3 layer remained intact up to an hour after immersion in 0.5 mol-% DIPA in DMSO, showing good etch selectivity between the As_2S_3 and the As_2Se_3 layer. Therefore, 0.5 mol-% DIPA in DMSO was used as the developer for all etch processing of As_2S_3-on-As_2Se_3 discussed below.

Ethanolamine was found to dissolve the as-deposited $Ge_5(As_2Se_3)_{95}$ material faster and left less residue than other amines. Ethanolamine, propylamine, and butylamine are known to dissolve thermally deposited Se containing ChG materials[10]. Visual observations revealed that ethanolamine dissolved the as-deposited $Ge_5(As_2Se_3)_{95}$ film in 60 minutes whereas it took propylamine and butylamine over 120 minutes to dissolve the material. SEM images taken after etch processing with propylamine and butylamine showed that undissolved material was still present on the surface. Ethanolamine was therefore used as the developer for all further etch processing of $Ge_5(As_2Se_3)_{95}$ films.

3.2. MPL of micro-structures

Dose arrays were used to study the exposure conditions needed to photo-pattern As_2S_3-on-As_2Se_3 and $Ge_5(As_2Se_3)_{95}$ films. The samples were exposed over a range of powers at a fixed scan speed to identify the minimum power needed to create robust features, the maximum power above which damage occurred, and how the feature size scaled with power. Dose arrays were photo-patterned in the As_2S_3-on-As_2Se_3 film over a range of average focused laser powers (0.02 mW – 1.00 mW) then etched in 0.5 mol-% DIPA in DMSO. Dose arrays were photo-patterned in the $Ge_5(As_2Se_3)_{95}$ film over a range of average focused laser powers (0.02 mW – 1.00 mW) then etched in Ethanolamine.

Micro-structures patterned in the As_2S_3-on-As_2Se_3 film possessed the intended cylindrical shape and height (2 μm based on the film thickness), as observed for prior exposures in multi-layered As_2S_3-on-As_2Se_3 film [4] (Fig. 1A,B). This is in sharp contrast to the beaded shapes observed for micro-structures patterned in single-layer As_2S_3 on Si substrate films [4]. The addition of the AR layer results in the absence of the standing-wave effect (SWE). This absence avoids intensity modulation and resulting "pinch-off" of the structure near the interface that is observed with the single-layer As_2S_3 on Si substrate films [4].

Micro-structures patterned in the $Ge_5(As_2Se_3)_{95}$ film possessed a pyramid shape and although the MPL patterning was expected to produce either cylindrical pillars or bead shaped pillar as observed in single-layered As_2S_3 (Fig. 1C,D). In addition, the height of the structures was ~ 250 nm whereas the intended height (film thickness) was 500 nm. The micro-structure shape and height depends on the influence of the SWE in the film, degree of cross-linking, and etch processing. Increased material cross-linking at the material-substrate interface may occur during thermal deposition on an uncooled sample stage. $Ge_5(As_2Se_3)_{95}$ is more resistant to amine-based etchants than As_2S_3 films. Therefore, a stronger amine based etchant must be used for Ge-doped As/Se films. Due to the strength of this etchant and the long times required to completely etch away the material (low etch rate), it is possible that some of the photo-patterned material is also etched (selectivity is decreased) and the height decreased and structure morphology altered. However, the pyramid shape may be good for a graded index AR coating.

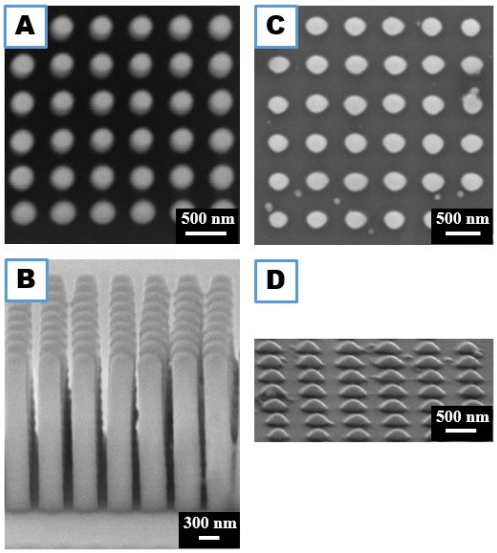

Figure 1. SEM images of (**A**) top-down and (**B**) profile micro-structures photo-patterned in As_2S_3-on-As_2Se_3 films. SEM images of (**C**) top-down and (**D**) profile micro-structures photo-patterned in $Ge_5(As_2Se_3)_{95}$ films.

Feature size increases with fabrication power for both the As_2S_3 on As_2Se_3 film and the $Ge_5(As_2Se_3)_{95}$ film, which is consistent with that typically found for photochemically thresholded process in photopolymers. In Fig. 2, the widths of the micro-structures photo-patterned in the As_2S_3-on-As_2Se_3 film were measured from SEM top-down images over a range of powers. The width measurements were used to create a plot of pillar widths versus power with error-bars indicating the standard deviation of those measurements (Fig. 2). The relationship between laser-patterned structure-width, spot size r_0, average laser power $\langle P \rangle$, and the threshold laser power for producing a feature $\langle P \rangle_{Th}$ can be described by equation 1 [11].

$$\text{structure-width} = \sqrt{2} r_0 \sqrt{\ln \frac{\langle P \rangle}{\langle P \rangle_{Th}}}, \quad (1)$$

In Fig. 2, the smooth curve is a global fit of the pillar widths to equation 1 with r_0 and $\langle P \rangle_{Th}$ set as free parameters. The fit suggests that a similar threshold related process occurs when photo-patterning in As_2S_3 and the $Ge_5(As_2Se_3)_{95}$ film as it does in photopolymers. The fit for the $Ge_5(As_2Se_3)_{95}$ structures is not as well defined as it is for

the As_2S_3 structures due to variability in $Ge_5(As_2Se_3)_{95}$ structure widths for a given array. This variability may be caused by difficulty in accurate top-down width measurements due to the pyramid shape nature of the structures. Additionally, the widths may vary across an array due to the high viscosity of the etchant and the potential for uneven material dissolution.

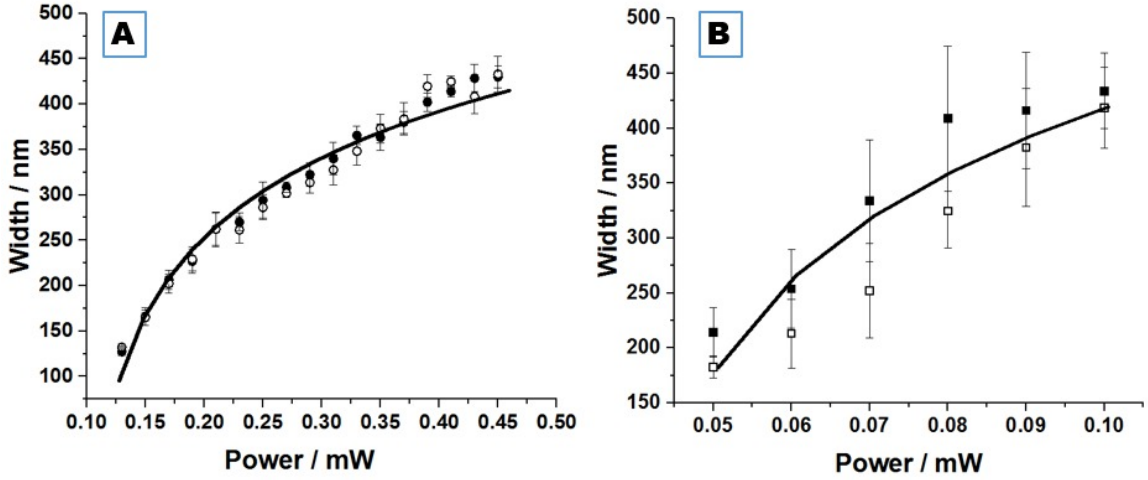

Figure 2. (**A**) X-width (filled shapes) and y-width (open shapes) measurements for structures patterned in As_2S_3-on-As_2Se_3 film (circles) versus average laser power. (B) X-width (filled shapes) and y-width (open shapes) measurements for structures patterned in $Ge_5(As_2Se_3)_{95}$ films (squares) versus average laser power.

$Ge_5(As_2Se_3)_{95}$ films are more photo-sensitive than As_2S_3 films. Features with widths of 200 nm are formed at an average power of 0.05 mW; however, to produce this sized feature in As_2S_3 a power of 0.18 mW is needed. Increased photo-sensitivity may occur as a result of the addition of Se and Ge into the material system. Increased Se content is known to red-shift the electronic band-edge of bulk $As_2S_{1-x}Se_x$ [12]. If the same can be expected for thermally deposited films, then thermally deposited films should exhibit higher photo-sensitivity as the Se content is increased. Additionally, Ge atoms are more polarizable than S atoms, and the electronic band-edge of bulk ChGs red-shifts with increasing Ge content [12]. By increasing the Ge content in thermally deposited films, the linear and nonlinear absorptivity should increase, making the film more photo-sensitive.

3.3. Micro-Raman characterization of unexposed films

The chemical bonding in pristine As_2S_3-on-As_2Se_3 and $Ge_5(As_2Se_3)_{95}$ films was investigated by micro-Raman spectroscopy. Thermal deposition fragments the material into molecular clusters which can be identified from the peaks in the Raman spectra [13, 14] (Fig. 3). For As_2S_3 films, molecular clusters of As_4S_6, As_4S_4, S_8, and other clusters containing homopolar As-As and S-S bonds are responsible for a film's photosensitivity [2, 13]. In $Ge_5(As_2Se_3)_{95}$ films, the presence of Se-Se may be responsible for the $Ge_5(As_2Se_3)_{95}$ films' increased photo-sensitivity over As_2S_3, as homopolar Se-Se bonds (192 kJ mol^{-1}) are weaker than S-S bonds (266 kJ mol^{-1}) [15].

3.4. Index of refraction for unexposed films

The index of refraction and extinction coefficient in unexposed As_2S_3-on-As_2Se_3 and $Ge_5(As_2Se_3)_{95}$ films were investigated by spectroscopic ellipsometry. The index of refraction and dispersion curve is approximately 0.500 units greater for Ge than As_2S_3 (Fig. 4). The extinction coefficient κ (not shown) has values at or near zero for both films. The increase in index and photo-sensitivity found in the $Ge_5(As_2Se_3)_{95}$ films over that of As_2S_3 film indicate that Ge/Se based films could be useful for high-index photonic devices.

3.5. Film degradation

Photo-patterned structure degradation was investigated in the $Ge_5(As_2Se_3)_{95}$ and As_2S_3 films and correlated with

the environmental conditions, age of the film, and its chemical composition. The surfaces of thermally deposited As_2S_3 films are known to become chemically altered and degraded due to exposure from light and water vapor [8]. The incorporation of Ge and Se into a system is expected to increase the stability of photo-patterned micro-structures [12]. Prior to MPL, films were kept in a petri dish wrapped with aluminum foil, and stored in an amber desiccator in a cupboard, to prevent exposure to ambient light and moisture. After MPL, the micro-structures were kept in a petri dish in a cupboard; however, they were not kept in the desiccator, leaving them exposed to ambient light and moisture. In order to observe and compare the degradation of both the $Ge_5(As_2Se_3)_{95}$ and As_2S_3 micro-structures, SEM imaging and EDX spectroscopy were used to evaluate the morphology and structure chemical composition over time.

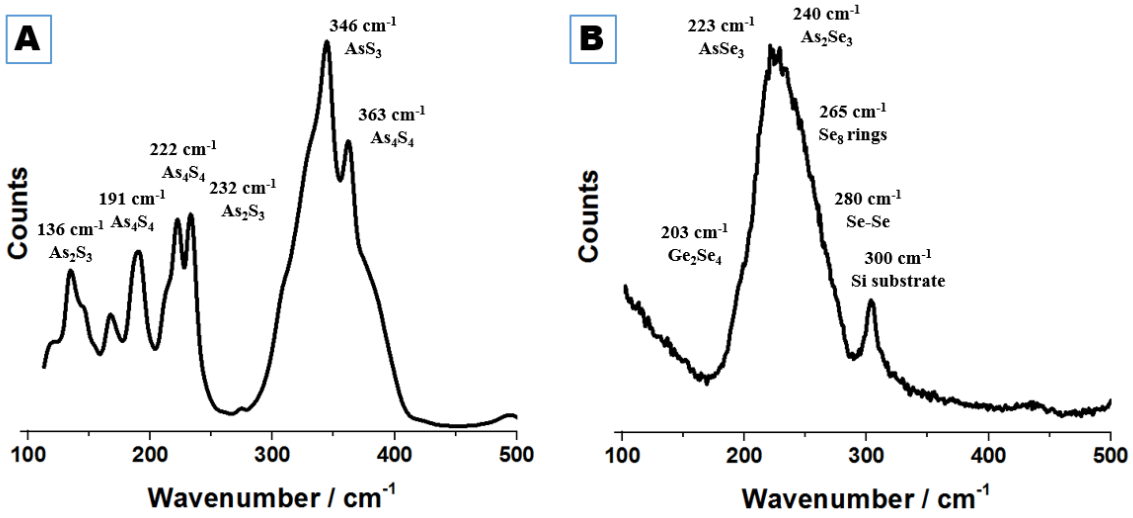

Figure 3. Raman spectra of (**A**) As_2S_3 film and (**B**) the $Ge_5(As_2Se_3)_{95}$ film with peaks identified.

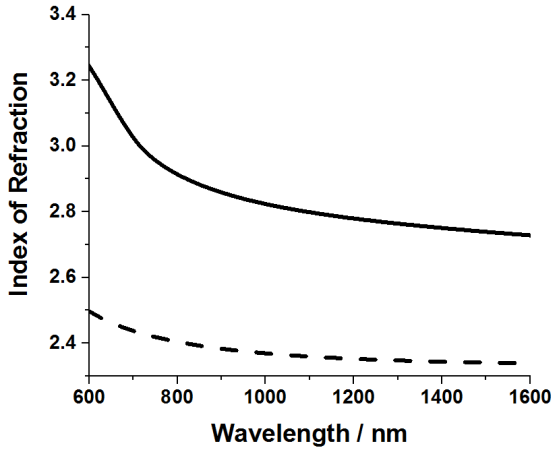

Figure 4. Optical properties of the films, as measured by ellipsometry. The index of refraction n for the pristine As_2S_3-on-As_2Se_3 film (dashed line) is compared to the index of refraction for the pristine $Ge_5(As_2Se_3)_{95}$ film (solid line). The extinction coefficient κ (not shown) has values at or near zero for both films.

The addition of Ge and Se into the composition stabilizes the film and decreases the degradation effects typical of As_2S_3 films. Micro-structures created by MPL in As_2S_3 are unstable and deteriorate with time. After 3 months of aging, the As_2S_3 micro-structures are found by SEM imaging to have deformed (Fig. 5). EDX spectroscopy confirms

this is due to a combination of crystallization and formation of As_2O_3. In comparison, after 3 months in the same environment, the $Ge_5(As_2Se_3)_{95}$ micro-structures remained unchanged (Fig. 1C,D). Ge-doped As/Se material is highly stable and therefore better suited for manufacturing compared to As_2S_3.

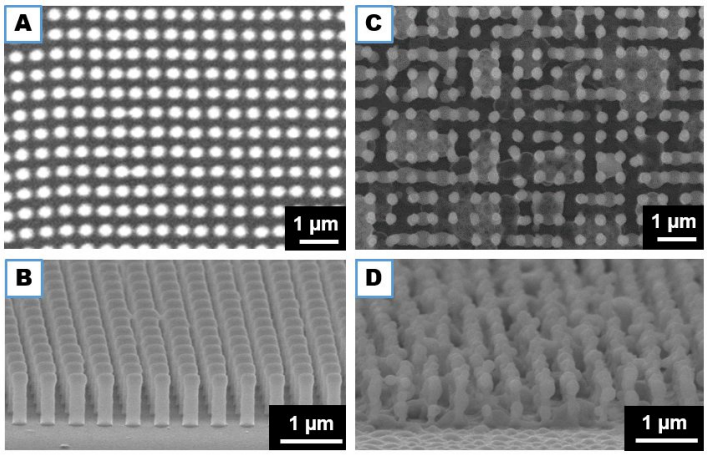

Figure 5. (**A**) Top-down and (**B**) side-view SEM images of nano-pillars fabricated by MPL in thermally deposited As_2S_3. (**C**) Top-down and (**D**) side-view images of the same structures after storing for three months in the dark and ambient air.

4. CONCLUSIONS

Thermally deposited As_2S_3-on-As_2Se_3 and $Ge_5(As_2Se_3)_{95}$ films were found to be photo-patternable by multi-photon lithography (MPL). MPL was used to photo-pattern micro-structures in Ge-doped As/Se films for the first time. $Ge_5(As_2Se_3)_{95}$ films were found to be more photo-sensitive than As_2S_3 films, and structures could be fabricated in the Ge films at a lower average power. The photo-patterned structures in the $Ge_5(As_2Se_3)_{95}$ films have a pyramid shape which may be useful for a creating graded index anti-reflective surfaces. The addition of Ge and Se in the $Ge_5(As_2Se_3)_{95}$ film stabilizes the film and decreases the degradation effects typical of As_2S_3 films. The high index, increased photo-sensitivity, and stable nature of the $Ge_5(As_2Se_3)_{95}$ film over the As_2S_3 films suggests that Ge/Se based chalcogenides may be a better route for the manufacturing of functional optical and photonic devices via MPL.

5. ACKNOWLEDGMENTS

This work was partially supported by NSF CAREER award DMR/CHE-0748712; Lockheed Martin; the Florida High Tech Corridor Council; the Space Research Initiative Program, through the Florida Space Institute hosted at the University of Central Florida; and the National Aeronautics and Space Administration through the University of Central Florida's NASA-Florida Space Grant Consortium. Anna Lewis was supported by a UCF SURF Scholarship. We thank Dr. Pieter Kik and Mr. Chatdanai Lumdee for assistance with the ellipsometry measurements.

6. REFERENCES

[1] Kuebler, S.M. and Rumi, M., "Nonlinear optics -- applications: three-dimensional microfabrication," Encyclopedia of Modern Optics, 189-206 (2004).

[2] Wong, S., Deubel, M., Perez-Willard, F., *et al.*, "Direct laser writing of three-dimensional photonic crystals with a complete photonic bandgap in chalcogenide glasses," Adv. Mater., 18(3), 265-269 (2006).

[3] Schwarz, C.M., Williams, H.E., Grabill, C.N., *et al.* "Processing and properties of arsenic trisulfide chalcogenide glasses for direct laser writing of 3D micro structures," Proc. SPIE 8974, 89740P-1 - 89740P-11, (2014).

[4] Schwarz, C.M., Grabill, C.N., Gleason, B., *et al.* "Fabrication and characterization of micro-structures created by direct laser writing in multi-layered chalcogenide glasses," Proc. SPIE 9374, 937403-1 - 937403-9, (2015).
[5] Hilton, A.R., Sr., *Chalcogenide Glasses for Infrared Optics*, McGraw-Hill Companies, Inc., New York City, 1-304 (2010).
[6] Nicoletti, E., Bulla, D., Luther-Davies, B., *et al.*, "Wide-angle stop-gap chalcogenide photonic crystals generated by direct multiple-line laser writing," Appl. Phys. B, 105(4), 847-850 (2011).
[7] Nicoletti, E., Bulla, D., Luther-Davies, B., *et al.*, "Generation of λ/12 nanowires in chalcogenide glasses," Nano. Lett., 11(10), 4218-4221 (2011).
[8] Allen, P.J., Johnson, B.R., and Riley, B.J., "Photo-oxidation of thermally evaporated As_2S_3 thin films," J Optoelectron Adv Mater, 7(4), 1759-1764 (2005).
[9] Park, J.K., Lee, J.H., Shin, S.Y., *et al.*, "Compositional dependence of hardness of Ge-Sb-Se glass for molded lens applications," Arch. Metall. Mater., 60(2), 1205-1208 (2015).
[10] Kumaresan, Y., Rammohan, A., Dwivedi, P.K., *et al.*, "Large area IR microlens arrays of chalcogenide glass photoresists by grayscale maskless lithography," Appl. Mater. Interfaces, 5, 7094-7100 (2013).
[11] Williams, H.E., "*Photophysical and photochemical factors affecting multi-photon direct laser writing using the cross-linkable epoxide SU-8*," in *Department of Chemistry*2013, University of Central Florida: Orlando, FL. p. 165.
[12] Su, X., Wang, R., Luther-Davies, B., *et al.*, "The dependence of photosensitivity on composition for thin films of $Ge_xAs_ySe_{1-x-y}$ chalcogenide glasses," Appl. Phys. A, 113, 575-581 (2013).
[13] Zoubir, A., Richardson, M., Rivero, C., *et al.*, "Direct femtosecond laser writing of waveguides in As_2S_3 thin films," Opt. Lett., 29(7), 748-750 (2004).
[14] Iovu, M.S., Kamitsos, E.I., Varsamis, C.P.E., *et al.*, "Raman spectra of As_xSe_{100-x} and $As_{40}Se_{60}$ glasses doped with metals," Chalcogenide Lett., 2(3), 21-25 (2005).
[15] Fairman, R. and Ushkov, B., *Semiconducting Chalcogenide Glass I: Glass Formation, Structure, and Simulated Transformations in Chalcogenide Glasses*, Vol. 78. Academic Press, San Diego (2004).